# Experimental study of the quasi-static and dynamic behaviour of cork under compressive loading

**Celina Pires Gameiro · José Cirne · Gérard Gary**

**Abstract** Cork is a natural cellular material with increasing industrial applications due to its remarkable combination of properties. Its mechanical behaviour explains why it is often used for applications like sealing, packaging, insulation, vibration control, weight reduction, flotation, sound damping, etc. However, the mechanical behaviour of cork when subjected to impact has not been well investigated yet since the studies described in the literature generally focus strain rates below $10^{-1}$ $s^{-1}$. Understanding the behaviour of cork at high rates of deformation becomes imperative when considering applications such as crash protection. Hence, in the present work, the authors compare the quasi-static and dynamic response of four types of cork when compressed axially at strain rates from $10^{-3}$ $s^{-1}$ to 600 $s^{-1}$. Data from the Split-Hopkinson Pressure Bars are used to generate stress–strain curves for natural and agglomerate cork samples, and the results are discussed in terms of the cellular structure of cork.

## Introduction

In the last few years, cellular materials have been playing a very important role in industrial applications

C. P. Gameiro (✉) · J. Cirne
CEMUC—Departamento de Engenharia Mecânica,
Faculdade de Ciências e Tecnologia da Universidade de
Coimbra, 3030-788 Coimbra, Portugal
e-mail: celina.gameiro@dem.uc.pt

G. Gary
Laboratoire de Mécanique des Solides, Ecole
Polytechnique, 91128 Palaiseau, France

because they may have good energy absorption capabilities, as well as important advantages such as damping, insulation, specific stiffness and fire retardant properties. Actually, under compressive loading, cellular materials can undergo large strains while maintaining a low stress level before the densification. Nevertheless, the properties of foams can vary significantly by the choice of the cell wall material, the volume fraction of the solid, the geometry and the strain rate of the loading. Hence, many authors have been trying to characterize those materials under quasi-static and dynamic loading [1–4].

Cork is a natural product that constitutes the outer bark of the cork oak (*Quercus suber*), which mainly grows in Portugal, Spain and Algeria. It is formed by cells disposed in successive layers, each layer corresponding to one year's growth. The first cork stripping is performed approximately after 30 years of life of the tree, and is usually done regularly every 9 years along the 150–200 years of average lifetime of the cork oak. Cork is a unique material, due to its low density, great elasticity, chemical stability and resilience, its no permeability to liquid and gases and its resistance to wear and fire. Besides, it is natural and ecological, hygienic, easy to maintain and a very durable material. That is why it is used today for example for thermal and acoustic insulation, as a seal and as an energy-absorbing medium in flooring, shoes and packaging. Nevertheless, cork is definitely a complex cellular material, with quite unknown or not well understood mechanical properties. The fundamental aspects of the static mechanical behaviour of cork under axial compressive loading have already been studied by several authors [5–7]. In particular, Gibson et al. [8] investigated in great detail the structure and cell wall deformation

**Fig. 1** Morphology of a cork cell (**a**) and aspect of the cork oak bark (**b**)
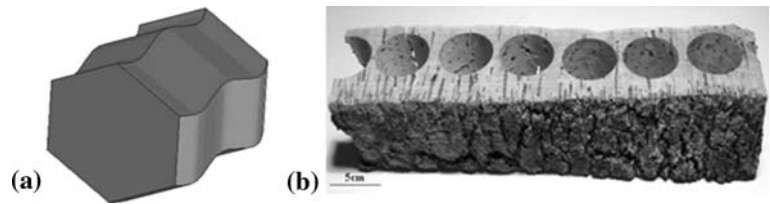


characteristics of cork when loaded, thus being able to compare the moduli and mechanical properties measured with theoretical expressions. However, the mechanical behaviour of cork when subjected to impact has not been well investigated yet since the studies described in the literature generally focus strain rates inferior to $10^{-1}\,s^{-1}$. As a consequence, the energy absorption potential of cork at different strain rates has neither been investigated nor evaluated yet. Such an understanding becomes imperative in applications such as crash protection, wherein the component has to withstand high rates of deformation. Moreover, cellular materials are increasingly being used in the automotive and military industry as a filler in tubular metallic structures, in order to increase the amount of specific energy absorbed during an impact. Cork, mainly in its agglomerate form, may also combine interesting mechanical properties adequate to its use as an innovative energy-absorbing material, applied alone or in combination with metallic components. Hence, this work pretends to be a start for the study of the mechanical behaviour of cork under impact loading. The quasi-static (at $10^{-3}\,s^{-1}$) and the dynamic behaviour of cork (strain rates from $200\,s^{-1}$ to $600\,s^{-1}$) were compared and the possible influence of the cork type, the density, the humidity, the cellular structure and the strain rate was examined.

## Experimental tests

### The cork structure

In order to characterize the cork structure, the authors usually refer to three principal directions which define the orientation of the material in the cork oak: directions along the radius and the axis of the trunk, respectively designated by radial, and axial, and tangential direction to the circumference. As with some other cellular materials, cork is composed of closed cells, which represent approximately 15% of the total volume of the material and form a three-dimensional structure in space [8]. The cells are described by three directions, respectively perpendicular to the three principal directions already defined, with electronic scanning devices [5]. The cork cells can be defined as

prisms, globally hexagonal, which form columns in the radial direction. The cell walls in this direction present significant corrugations, so that the cells are shaped like a concertina (Fig. 1(a)).

One of the major problems related to the characterization of natural cork is the complexity of the cells shape, as the cells walls do not have a uniform thickness, height, or geometry. Those parameters vary as a function of the cork oak considered, of the defects detected in the bark, and even a same piece of cork presents different types of cells depending on the season their growth took place (a piece of cork contains a fraction of spring cells and a fraction of autumn cells with different characteristics and porosities). Globally, the cells have an average thickness of 1 μm, a height of about 45 μm and an hexagonal face-edge of approximately 20 μm.

### Materials

The particular structure of the cork, as a consequence of the cork cells shape, explains the choice of the samples used for the quasi-static and dynamic uniaxial compressive tests. Hence, the specimens used were removed from the cork oak in the radial direction and in another of the two non-radial directions because a similar compressive behaviour may be expected in the axial and tangential directions.

For the static and dynamic tests, natural radial (R) and non-radial (NR) cork cylinders, as well as agglomerate (A) and micro-agglomerate (MA) cylindrical cork samples were used. The objective of this choice was to compare the performance of agglomerate material, produced industrially and available in many shapes and sizes, with the behaviour of a natural material characterized by much more variable properties and which is more difficult to use in industrial applications because of its shorter size. The agglomerate cork tested is called "composed agglomerate" and is made of 3–6 mm cork particles mixed with polyurethane adhesive, latex, paraffinic oil and paraffin. The micro-agglomerate cork contains smaller 0.5 mm to 2 mm cork particles.

The cork samples produced by ROCAP were cylinders with an average diameter of 22.8 mm and an average length of 51.0 mm, except the radial cork cylinders which could not have a length higher than

26.2 mm because they were removed from the interior to the exterior of the bark (Fig. 1(b)). Moreover, all the natural cork cylinders were extracted from the same cork oak, or from neighbour cork oaks, in order to limit as much as possible the variations of the structure and of the quality of the cork.

An automatic system from EGITRON, called "Medcork", used for the measurement of cork stoppers, was used to register the length, the average diameter, the ovality, the density and the humidity of each sample. Some discs of radial cork were also provided: some had an approximate diameter of 35 mm and a thickness of 7 mm, whereas others had an approximate diameter of 27 mm and a thickness of 6 mm. For technical reasons, inherent to the fact that the Medcork is not prepared for short cylinders, the values of humidity and ovality for the discs were not displayed. After the measurements, some of the specimens were cut out from the cylinders, according to the needs of the tests performed, and weighed again.

Quasi-static tests

The quasi-static uniaxial compressive tests on cork were performed in the hydraulic testing machine INSTRON 4206 available in our laboratories, with a load cell capacity of 100 KN. The relative uncertainty of this cell was of approximately 0.226% in the force range from 0 KN to 2 KN. Thus, the accuracy of the results obtained was guaranteed even for low stresses measurements. The loading speed was fixed at 1.5 mm/min. Hence, 15 mm and 20 mm length cylinders of radial, non-radial, agglomerate and micro-agglomerate cork were tested at strain rates of $1.6 \times 10^{-3}$ s$^{-1}$ and $1.25 \times 10^{-3}$ s$^{-1}$.

A list of all the specimens tested with the hydraulic testing machine was established, specifying the corresponding geometry, weigh and Medcork characteristics. At least three experiments were conducted for each specimen length and type of cork.

Dynamic tests

*Brief introduction to the Split Hopkinson Pressure Bars (SHPB)*

The cork samples were dynamically tested on Split Hopkinson Pressure Bars. The SHPB (Split Hopkinson Pressure Bar) system, also called Kolsky's apparatus, is a commonly used experimental technique in the study of constitutive laws of materials at high strain rates. The first use of a long thin bar to measure stresses under impact conditions has been reported in [9]. The experimental setting with two long bars widely used today was pioneered by Kolsky [10].

A typical SHPB test system is shown in Fig. 2. It is composed of the long input and output bars with a short specimen placed between them. With the impact of a projectile at the free end of the input bar, a compressive longitudinal "incident" wave $\varepsilon_i(t)$ is created in the input bar. Once the incident wave reaches the interface specimen-bar, a reflected pulse $\varepsilon_r(t)$ in the input bar and a transmitted pulse $\varepsilon_t(t)$ in the output bar are developed. With gages glued on the input and output bars (A and B), these three basic waves are recorded. Their processing allows for the knowledge of forces and particle velocities at both faces of the specimen.

*Brief recall of the basic processing technique*

As the incident and the reflected wave have to be both known, the optimal position of a single gauge station "A" that allows for the longest loading time is the middle of the input bar. The maximal theoretical length of the striker is then half of the input bar. In fact, because of the non-zero rise time of the incident wave, its length is more often around 80% of the theoretical one.

What is needed is the value of forces and particle velocities at specimen faces. They are calculated with waves shifted at the same points. For slender elastic bars, it is assumed that elastic waves propagate without dispersion and they are simply time shifted to bar ends.

Let us call $\varepsilon_i(t)$, $\varepsilon_r(t)$ and $\varepsilon_t(t)$ the corresponding (shifted) waves. For sake of simplicity, with the one-dimensional analysis, usual relations between jumps of stress ($\Delta\sigma$), particle velocity ($\Delta v$) and strain ($\Delta\varepsilon$) are used.

$$\Delta\sigma = -\rho C \Delta v, \quad \Delta v = -C \Delta\varepsilon \qquad (1)$$

Using Equations (1) together with the superposition principle, the velocities and forces at both specimen faces are given by the formulae (2) and (3).

**Fig. 2** Split Hopkinson Pressure Bars used to perform the dynamic tests
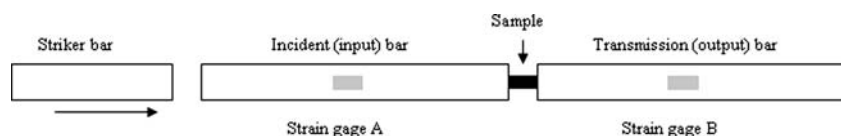
$$V_i(t) = -c(\varepsilon_i(t) - \varepsilon_r(t))$$
$$V_o(t) = -c\varepsilon_t(t) \qquad (2)$$

$$F_i(t) = S_b E(\varepsilon_i(t) + \varepsilon_r(t))$$
$$F_o(t) = S_b E \varepsilon_t(t) \qquad (3)$$

where $V$ is the velocity, $F$ is the force, $S_b$ is the area of the bars, $E$ is the Young's modulus of the bars and $c$ is the wave speed in bars. Subscripts i and o indicate the input and output side, respectively.

Assuming that the stresses and the strains are homogeneous in the specimen, the average strain, the average strain rate and the average stress in the specimen, as a function of time, are given by the expressions (4), where $l_S$ and $S_S$, respectively, stand for the specimen length and cross-sectional area, and $U$ is the displacement of the interface considered.

$$\bar{\varepsilon}(t) = \frac{U_i(t) - U_o(t)}{l_S}$$
$$\bar{\dot{\varepsilon}}(t) = \frac{V_i(t) - V_o(t)}{l_s} \qquad (4)$$
$$\bar{\sigma}(t) = \frac{F_i(t) + F_o(t)}{2S_S}$$

These equations correspond to the standard analysis of the test [11]. It appears that the equilibrium of forces can be verified for each test, using expressions (3), and one can assume the hypothesis of homogeneity of stresses and strains in the specimen only when the forces at the sample interface are equal.

*Present device and processing technique*

An important point is to verify the adequate adaptation of the impedance of the bars and the sample, and that of the measured forces to the stiffness of the bars, so that the waves amplitudes in the input and output bars (Fig. 3) can be great enough to calculate the forces and the velocities with accuracy. Hence, and particularly for the dynamic study of cellular materials with Hopkinson Bars, viscoelastic bars are used.

The SHPB set-up (striker, input bar and transmitter bar) used here is made of Nylon bars with a diameter of 40 mm. The striker is 1 m long, the input bar 3 m and the output bar 2 m. Strains at points A and B are measured with strain gauges. Assuming a uniaxial stress state and plane waves at gauges stations, an improved measurement of the strain is made by using a complete gauge bridge with each couple of transverse
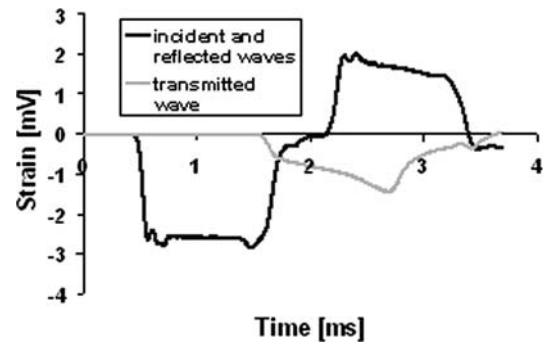


**Fig. 3** Example of recorded waves for cork

and longitudinal gauge diametrically opposed on the surface of the bar to eliminate a possible bending component. It is made with longitudinal and transverse gauges (2 mm, Kyowa—KSN-2-120-F3-11), where the transverse strain is equal to the longitudinal strain multiplied by Poisson's ratio. The bridge is supplied by a monitored 2 V tension and the signals are amplified (amplifier gain 100–200–500–1000, six channels, passing band 200 kHz). They are then recorded with a data acquisition card (12 bits) with the time base set at the value of 1 μs. Knowing that wave speed in nylon bars is approximately 1,820 m/s, it is simply deduced from the dimensions of the set up that the loading pulse duration is around 1.1 ms. Thus, the time of loading $\tau$ applied to the specimen is related to the striker length $l_{striker}$ and determines the maximum strain $\varepsilon_{max}$ considered in the sample for a given strain rate (expressions (5) and (6)).

$$\tau = \frac{2l_{striker}}{C_0} \qquad (5)$$

$$\varepsilon_{max} = \dot{\varepsilon}\tau \qquad (6)$$

The shifting of waves to specimen ends takes account of the dispersion (which means that the speed of the waves depends slightly on their frequency) and for damping. The authors use a dispersion relation that is the first mode solution of Pochhammer [12] and Chree [13] equation, generalised to the case of viscoelastic bars by Zhao and Gary [14], as it is needed in the present paper.

For all the samples tested dynamically in SHPB, the authors used the software DAVID$^{TM}$, created in the LMS, *Laboratoire de Mécanique des Solides* (*Ecole Polytechnique, France*) by G. Gary and V. De Greef, to process the results and obtain the stress–strain curves. It allows for an easy check of forces for each test and a good equilibrium was observed
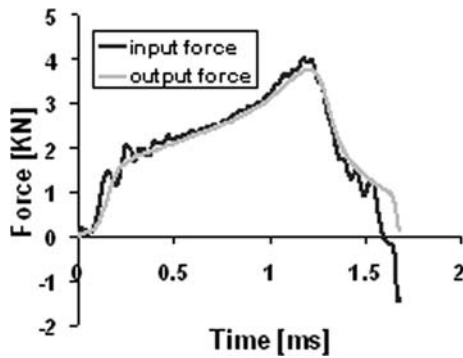
**Fig. 4** Equilibrium of the input and output forces at the interfaces of the samples

considering both forces applied to specimen faces (Fig. 4). Checking this equilibrium ensures a good homogeneity of the stress state; the strain state homogeneity needs, at least, a positive strain-hardening response of the material.

*Description of the tests*

As referred to above, cork disks of the four types were tested on nylon SHPB (Fig. 5). The distance strain gage/sample was 1.55 m for the input bar and 0.394 m for the output bar. The nylon striker was expelled at 3 m/s and 6 m/s approximately, and originated several average strain rates in the samples, from 200 s$^{-1}$ to 600 s$^{-1}$.

Figure 6 shows the variations of the strain rate measured with the sample strain during the test. The strain rate considered as a reference for each test is the mean value obtained in the strain range corresponding to the plateau stress. As for the quasi-static tests, the dimensions and Medcork properties of the samples tested with nylon SHPB, as well as the strain rate originated in each one of them, were registered.

Some of the samples were also impacted twice to analyse the effect of a second loading on the material stress–strain response.
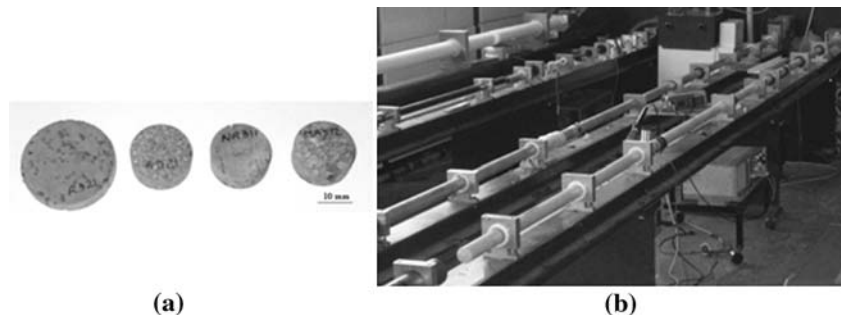
## Results and discussion

Quasi-static tests

Independently of the cork type, Medcork properties (humidity, ovality, density) and length of each specimen, the quasi-static curves obtained for each series of three samples are identical. Figure 7 illustrates the average stress–strain curves obtained for each type of cork, up to 30% and 60% nominal strain. Each curve presents an elastic part, mainly as a result of the cell walls and edges bending. After that, elastic collapse gives an almost horizontal plateau for a stress of approximately 1 MPa: the cells collapse is mainly due to cells walls crushing. Actually, a real horizontal plateau does not exist (the stress grows slightly during the collapse propagation in cork) due to the structure heterogeneity. Finally, the complete collapse of the cells causes the curve to rise steeply at about 70% strain, when the cell walls start to touch each other. Large compressive strains are possible, absorbing a great amount of energy as the cells progressively collapse.

It appears that the static Young's modulus of radial and non-radial cork is higher than the one of agglomerate and micro-agglomerate cork. The static Young's modulus values are estimated to be 29 MPa for radial and 19 MPa for non-radial cork. Fortes et al. [5] refer to an increase of the modulus with density. Nevertheless, in this work, the discrepancy between density values of the samples tested seem to be insufficient to show this tendency. For low strains, natural cork (radial in particular) exhibits larger values of stress, but after 30% strain, the agglomerate, in particular micro-agglomerate cork, are more resistant.

The discrepancies observed in the stress–strain curves between radial and non-radial cork may be linked to the deformation mechanisms of the cork cells. Indeed, when cork is loaded in the non-radial direction, the cells start bending until they reach a critical
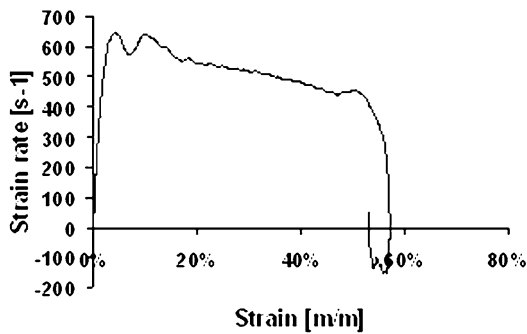
**Fig. 5** Geometry of the cork disks tested at high strain rates (**a**) and nylon Hopkinson Bars of the LMS (**b**)



(a)                                                                  (b)

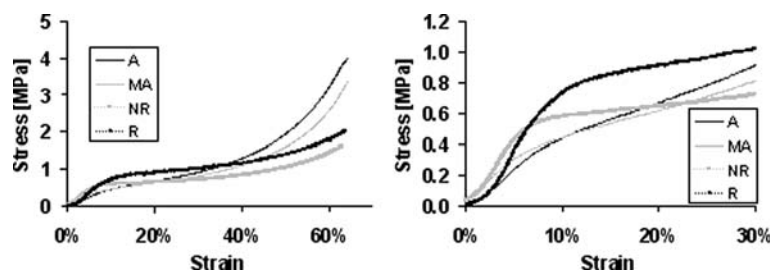**Fig. 6** Example of variation of the strain rate with strain in a cork sample

stress. At that point, they collapse by elastic buckling, responsible for the existence of the plateau stress. Finally, at high strains, the opposing cell walls touch leading to the deformation of the cell material itself. However, when the cork is loaded in the radial direction, the initial linear-elastic deformation involves axial or shear deformations of the cell walls themselves, while final failure is by tearing or crushing. Consequently, the radial stiffness and strengths are much larger than the non-radial ones, which only involve cell walls bending.

Gibson et al. [8] worked out in great detail how the behaviour of cork was linked to the cell wall deformation, considering the in-plane and out-of-plane deformation of an array of hexagonal cells. The material was treated as a structure made up of rigidly connected elastic beams that bend and buckle when the material is loaded. They calculated analytically, among other parameters, the Young's modulus and compressive collapse stress of cork, in the radial and non-radial directions, using the expressions (7) to (9), where $E_S$ and $\rho_S$ are the modulus and density of the cells wall material, $\rho$ is the overall density of cork, $t$ is the corrugated cell wall thickness and $a$ is the corrugation amplitude.

Non-radial Young modulus:

$$E_{NR} = 0.5 E_S \left(\frac{\rho}{\rho_S}\right)^3 \tag{7}$$

Radial Young modulus:

$$E_R = 0.7 E_S \left(\frac{\rho}{\rho_S}\right) \left(\frac{1}{1 + 6\left(\frac{a}{t}\right)^2}\right) \tag{8}$$

Non-radial and radial compressive collapse stress:

$$\sigma_{NR} = 0.05 E_S \left(\frac{\rho}{\rho_S}\right)^3 \approx \sigma_R \tag{9}$$

Adopting the values estimated by Gibson et al. [8] ($\rho_S = 1150$ kg/m$^3$; $E_S = 9$ GN/m$^2$; $t = 1$ μm and $a = 2.8$ μm) and considering that the overall density of the natural cork tested is approximately 185 kg/m$^3$, the above expressions lead to the results of expression (10).

$$\begin{cases} E_{NR} \approx 18.7 \text{ MPa} \\ E_R \approx 21.1 \text{ MPa} \\ \sigma_{NR} \approx \sigma_R \approx 1.8 \text{ MPa} \end{cases} \tag{10}$$

These values are quite in agreement with the measured moduli and stresses, specially the non-radial modulus. Obviously, the differences in the compressive collapse stresses were predictable as this approach does not account for natural variations in microstructure such as in the arrangement and morphology of the cell walls, cell walls thickness and cell wall material properties. Physically, the strains suffer a wider distribution than in idealized honeycombs, inducing increased bending moments and leading to a reduction in strength. Concerning the radial modulus, variations in the cells shape and corrugations may also explain why the measured value is higher than the calculated one.

Furthermore, in order to analyse the deformation uniformity in the natural cork samples statically tested, a regular grid was drawn in one of the samples. During the test, a progressive distortion of the grid was observed, demonstrating that deformation is not uniform, mainly near to the cracks and pores which constitute the lenticular channels and whose distribution in cork is irregular (Fig. 8). The existence of defects, missing cell walls and cell heterogeneities may
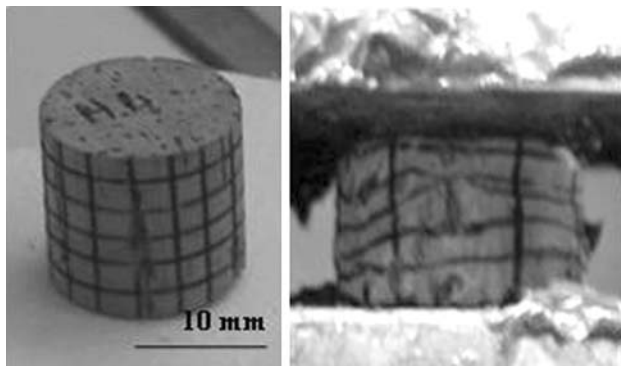
**Fig. 7** Average quasi-static compressive stress–strain curves for each type of cork, up to 60% and 30% strain

**Fig. 8** Evidence of the non-uniformity of the deformation of natural cork

be one of the causes of modifications in the patterns of failure and can affect the moduli and strength of cork. However, the quasi-static deformation of the agglomerate cork samples was quite uniform. The presence of the adhesive manages to homogenize and reinforce the cohesion of the material, so that its strength is larger than the one of natural cork at high strains, as depicted in Fig. 7.

Dynamic tests

Figure 9 shows the dynamic stress–strain curves for each type of cork samples. Agglomerate cork as well as micro-agglomerate cork present similar values, regardless of the sample tested characteristics and of the strain rate. These observations allow concluding that the variation of strain rate, for the dynamic range considered ($200~s^{-1}$ and $600~s^{-1}$), does not have an influence on the mechanical behaviour of the agglomerates. However, the dynamic plateau stress is larger than the static one, so agglomerates are not at all materials whose behaviour is independent from the strain rate applied.

Regarding non-radial and radial cork, the differences between quasi-static and dynamic results are much more significant. For non-radial cork, the value of the plateau stress varies with the sample, between 1 MPa and 1.5 MPa. There is no evidence of a direct relation between the plateau stress and the strain rate, since some non-radial samples such as NRD12 and NRD14 present the highest value of plateau stress in spite of being tested at the lowest strain rate values. The relevant points seem to be the microstructure and the properties of the tested sample. Indeed, the samples which present similar plateau stress (and similar stress–strain curves) are those which were cut out from the same initial cylinder (thus having the same Medcork reference). Hence, the authors can conclude that there may be a strong influence of the microstructure on the mechanical behaviour since samples made of neighbour cells present the same mechanical curve. As a consequence, the exact prevision of the dynamic behaviour of any sample of natural cork under compressive loading seems to be a major difficulty, mainly because cork microstructure varies with the region of

**Fig. 9** Dynamic stress–strain curves for the series of cork samples of each type. Comparison with the average quasi-static response
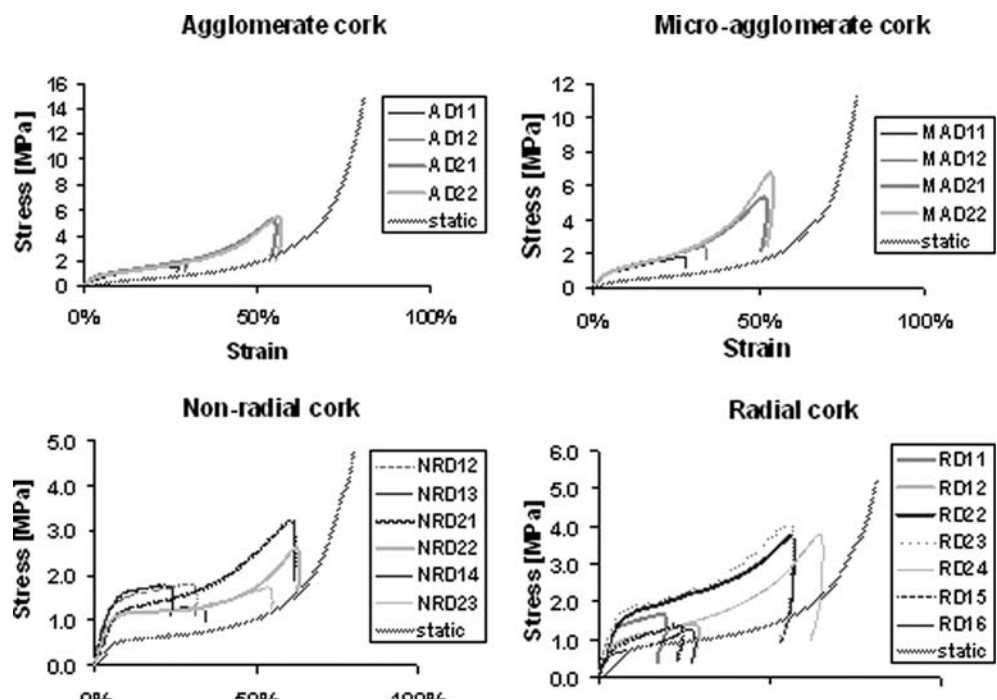
the cork oaks plantation, with the cork oak, and even in the same cork oak. In fact, the thickness, the inclination, and the number of corrugations in the cells can be relevant for its mechanical behaviour. Moreover, the high variability of density values can be affected by humidity and also depend on the cork type. Density gradients can be present on the same piece of cork: autumn and spring cells also have different shapes and thicknesses.

For radial cork, the plateau stress varies from 0.5 MPa to 2 MPa approximately. This cork type also presents the same results for samples obtained from the same original specimen, which may suggest that, once more, the mechanical behaviour of radial cork depends on the microstructure. However, there does not seem to be a linear influence of the samples density or humidity on their mechanical behaviour.

Comparatively with the quasi-static behaviour, non-radial cork presents a higher dynamic plateau stress. However, radial cork seems to have a slightly different behaviour since the increase of the plateau stress is not observed for all the samples tested. Some of them, such as RD16, present a plateau stress equal to the quasi-static one, certainly due to the concertina shape of the cells in that plane which affects the buckling modes of cell deformation.

Different contributions may explain the increase of the overall stress–strain response in the dynamic range. First of all, the cork may inherit the strain-dependence properties of the polymeric cell walls material, which mainly consists of suberin, lignin and cellulose. For obvious reasons, those properties are completely unknown and no conclusions can be raised on the walls material contributions. Besides, at high strain rates, three different features unique to the dynamic crushing of cellular solids can drive the cork strength upwards. The first is localisation, which consists of the existence of local strain rates much larger than the apparent nominal strain rate, in thin layers adjacent to the impact surface. The cells near the loading face are more tightly compressed causing the crushing strength to increase. The second is micro-inertia, associated with the rotation and lateral motion of the cell walls when they buckle. This feature tends to suppress the more compliant asymmetric buckling modes of cell deformation and diffuses the crushing wave front so that the strength reaches larger values. Under dynamic loading, the collapse mode may switch from the quasi-static mode to a new mode involving additional stretching which dissipates more energy [15]. Finally, densification at high strain rates can lead to a shock enhancement that is overdriven due to the cells collapse, resulting in the substantial increase of the forces transmitted.

Figure 10 shows the difference between the stress–strain curves obtained for each type of cork, when impacted twice at the same strain rate. Radial cork is the only type of cork, which exhibits a similar response after the second impact. It suggests that, to some extent, the particular shape of the corrugated cells on
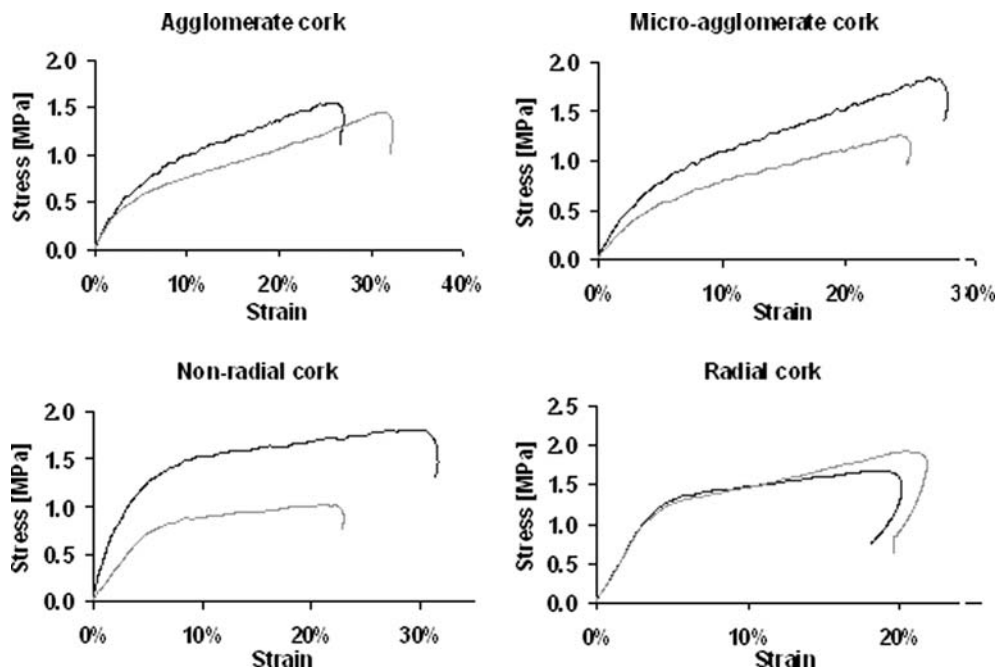


**Fig. 10** Stress–strain curves for a single and double impact on the same cork sample. The grey curve represents the cork response after the second shot

the radial direction contributes to preserve the integrity of the material, leading to the recovery of the cell walls deflexions after the impact.

## Conclusion

The dynamic behaviour of four types of cork has been observed, studied experimentally and compared with quasi-static compressive results. This is only the start of a major study focussed on the cork behaviour under impact loading and on the possible use of cork-based materials in innovative applications. Indeed, there are still many application fields that have not been explored yet for the use of cork, possibly due to the fact that it is a complex cellular material, characterized by highly variable mechanical properties, which clearly depend on its microstructure. This work highlighted some of its unknown mechanical aspects and suggested this biodegradable, cheap, light, energy-absorbing and unique material may be used in industrial applications involving impact loading, mainly in the agglomerate form. It also brought up the major difficulties related to the possible use and validation of constitutive laws for cork.

## References

1. Gibson LJ, Ashby MF (1997) Cellular solids: structure and properties. Cambridge University Press, Cambridge, UK
2. Deshpande VS, Fleck NA (2000) Int J Impact Engng 24:277
3. Paul A, Ramamurty U (2000) Mat Sci Eng A Struct A281:1
4. Santosa P, Wierzbicki T, Hanssen AG, Langseth M (2000) Int J Impact Engng 24:509
5. Fortes MA, Rosa ME, Pereira H (2004) A Cortiça. IST Press, Lisboa
6. Anjos O, Pina P, Rosa ME (1997) In: Proceedings of European conference on cork oak and cork. Centro de Estudos Florestais—Instituto Superior de Agronomia, Lisboa, p 317
7. Fortes MA, Nogueira MT (1989) Mat Sci Eng A Struct A122:227
8. Gibson LJ, Easterling KE, Ashby MF (1981) Proc R Soc Lond A377:99
9. Hopkinson B (1914) Phil Trans R Soc Lond A213:437
10. Kolsky H (1949) Proc R Soc Lond B 62:676
11. Gary G (2001) In: Nowacki WK, Klepaczko JR (eds) Trends in mechanics of materials, vol 3, Poland, p 179
12. Pochhammer L (1876) J für die Reine Angewandte Mathematik 81:324
13. Chree C (1889) Cambridge Phil Soc 14:250
14. Zhao H, Gary G, Klepaczko JR (1997) Int J Impact Engng 19:310
15. Klintworth JW (1989) Dynamic crushing of cellular solids (PhD Thesis, Department of Engineering, University of Cambridge